Journal of Applied Polymer Science

Multiresponsive Polyanionic Microgels with Inverse pH Responsive Behavior by Encapsulation of Polycationic Nanogels

Jennifer M. Knipe,[1] Frances Chen,[1] Nicholas A. Peppas[1,2,3]

[1]Department of Chemical Engineering, C0400, The University of Texas at Austin, Austin, Texas 78712
[2]Department of Biomedical Engineering, C0800, The University of Texas at Austin, Austin, Texas 78712
[3]College of Pharmacy, C0400, The University of Texas at Austin, Austin, Texas 78712
Correspondence to: N. A. Peppas (E-mail: peppas@che.utexas.edu)

ABSTRACT: Intelligent, stimuli-responsive hydrogels have great utility in various fields spanning biomedical technology, separations, and catalysis. Their overall response to surrounding fluids may be further tailored to a specific application by incorporation of one or more intelligent responses within one material, known as multiresponsive hydrogels. This is a report on the facile synthesis and characterization of poly(methacrylic acid-*co*-*N*-vinylpyrrolidone) microgels encapsulating polycationic nanogels (70–100 nm) to incorporate inverse pH responsive behavior within a single hydrogel. Potentiometric titration and pH swelling studies reveal a swelling response dependent on both pH and crosslinking agent. Additionally, a protein and a small molecule are loaded and released to evaluate the pH-dependent binding affinity. Such a material could exhibit unique protein-binding capacity and pH-responsive behavior for use in separation or drug delivery applications. © 2013 Wiley Periodicals, Inc. J. Appl. Polym. Sci. **2014**, *131*, 40098.

KEYWORDS: stimuli-sensitive polymers; hydrophilic polymers; proteins; biomaterials; microgels

Received 19 August 2013; accepted 21 October 2013
DOI: 10.1002/app.40098

INTRODUCTION

Stimuli-responsive hydrogels are three-dimensional, crosslinked polymer networks that respond in an intelligent manner to environmental changes such as pH, temperature, or analyte concentration while maintaining structural integrity.[1,2] Stimuli-responsive hydrogels may exhibit change in shape, surface characteristics, solubility, permeability, mechanical strength, or molecular self-assembly.[2,3] The specific response of the polymer network may be controlled by incorporation of functionalities such as chain side groups, branches, and crosslinks.[1]

In the case of pH-responsive hydrogels, the polymer network contains weak acid or base pendant groups that become ionized as a function of pH, ionic strength, and ionic composition, among other factors.[4] Additionally, changes in the pH of the environment will affect the porosity of the hydrogel; polyanionic hydrogels will be deswollen at low pH and swollen at high pH while the opposite is true for polycationic hydrogels.[5] These polymers are categorized as polyelectrolytes when they contain many ionizable pendant groups.[6]

These hydrogels have been studied for a number of applications, including controlled drug delivery,[5–10] biosensors,[11–13] tissue engineering,[14,15] catalysis,[16,17] and separations.[18,19] Such polyelectrolytes may be used within separation processes[10] as semipermeable membranes for counter-ions[1] or to separate and recover target proteins by phase separation or sorption by electrostatic or hydrophilic interactions.[20–22]

Recent developments with "intelligent" hydrogels have focused on the combination of multiple responsive properties to achieve a unique physiochemical response for specific applications.[23–26] In many instances, this hybrid is achieved by incorporating nanoparticles within polyelectrolytes.[17,27] These hybrid morphologies, such as multilayer and core-shell particles, are promising tools for drug delivery, theranostics, and binding and immobilization of proteins.[28–32]

In this article, we show the facile synthesis and characterization of polycationic nanogels encapsulated within polyanionic microgels. Previously within our lab, hydrophilic microgels with domains of hydrophobic nanogels were developed for the delivery of hydrophobic chemotherapeutics.[27] Building upon this idea, polycationic nanogels were incorporated into the polymerization of polyanionic microgels to achieve a system encompassing inverse pH-responsive behavior. Basic polymer characterization, including scanning electron microscopy (SEM), Fourier transform infrared spectroscopy (FTIR), and thermogravimetric analysis (TGA), was completed. Additionally, the pH response was evaluated by dynamic and equilibrium swelling experiments as a function of pH as well as

potentiometric titration. A cell proliferation assay and protein/small molecule loading and release were determined for drug delivery or protein separation applications.

EXPERIMENTAL

Materials

Methacrylic acid (MAA), *N*-vinyl pyrrolidone (NVP), and tetra(ethylene glycol) dimethacrylate (TEGDMA) were obtained from Sigma-Aldrich (St. Louis, MO). Poly(ethylene glycol) (400) dimethacrylate (PEGDMA) was purchased from Polysciences (Warrington, PA). Irgacure 184® (1-hydroxy-cyclohexyl-phenylketone) was purchased from Sigma-Aldrich. All reagents were used as received. Polycationic nanogels were synthesized as described previously.[8]

Synthesis of P(MAA-*co*-NVP) Hydrogels

P(MAA-*co*-NVP) hydrogels were synthesized by photoinitiated, free-radical polymerization. MAA and NVP were added at a 1:1 molar ratio to a 1:1 (w/w) deionized water and ethanol solution to yield a 1:1 (w/w) total monomer to solvent ratio. Polycationic nanogels were added to the solution at 0, 1, 2, or 5 wt% with respect to total monomer weight. One of two crosslinking agents, TEGDMA or PEGDMA, was added at 1 mol% of the total monomer molar content. Photoinitiator Irgacure 184® was added at 1 wt% with respect to total monomer weight.

The mixture was homogenized by sonication, then loaded into a sealed glove box (MBraun, Garching, Germany). The solution was purged with nitrogen for 10 min, then pipetted between glass slides ($150 \times 150 \times 3$ mm^3) separated by a Teflon spacer (0.7 mm). The plates were exposed to UV light (Dymax 2000-EC Light Curing System, Torrington, CT) at 70% intensity and allowed to polymerize for 30 min. Following polymerization, the film was removed from the slides and purified from unreacted reagents in deionized water for 7 days with daily water changes. The purified film was dried under vacuum at 30°C for 2 days. The dried film was crushed into particles <75 μm in size using a mortar and pestle and stored in a desiccator at room temperature.

Characterization

Scanning Electron Microscopy. SEM samples were prepared by dusting carbon tape-covered aluminum stubs with vacuum-dried, crushed microgels. The samples were coated with 12–15 nm of Pt/Pd coating using a Cressington 208 Benchtop sputter coater (Watford, England, UK). SEM images were obtained using an FEI Quanta 650 FEG scanning electron microscope (Hillsboro, OR).

Fluorescent Microscopy. Polycationic nanogels containing a monomer with primary amines were reacted with 4-chloro-7-nitrobenzofurazan (NBD-Cl, 98%) (Sigma-Aldrich), which generates a fluorescent product upon reaction with amines present on the surface of the nanogels. Nanogel presence within the microgels was then confirmed using a Zeiss Axiovert 200 M fluorescence microscope (Thornwood, NY).

Fourier Transform Infrared Spectroscopy. FTIR spectra for each sample were obtained using a Thermo Mattson Infinity Gold spectrometer (Thermo Fisher Scientific, Waltham, MA). Samples were pressed in KBr (Sigma-Aldrich) disks. For all formulations, background spectra were subtracted from the sample spectra. Copolymer compositions were calculated using a standard band of 650 cm^{-1} according to the calculation procedure reported previously.[33] Characteristic absorption bands of 1290 cm^{-1} and 2983 cm^{-1} were used as analytical bands for NVP and MAA, respectively.

Thermogravimetric Analysis. TGA was performed using a Mettler-Toledo TGA/DSC 1 (Columbus, OH). Samples were loaded in aluminum oxide crucibles. Temperature increased from 40 to 600°C at a rate of 10°C/min under nitrogen flowing at 50 mL/min.

Swelling Studies. Dynamic swelling studies were carried out in 0.1 M 3,3-dimethylglutaric acid/NaOH buffers ranging in pH from 3.2 to 7.6; pH 1.2 and 2.2 buffers were achieved using 3,3-dimethylglutaric acid/HCl and were stable during the relevant timescale. All buffers had an ionic strength of 0.1 M by addition of NaCl and were heated to 37°C. Hydrogel disks of 10 mm in diameter were stepped through each buffer from lowest to highest pH, spending 10 min in each buffer. The weights of the disks were measured between each buffer.

Equilibrium swelling studies were completed using a 0.1 N HCl solution and pH 7.4 phosphate-buffered saline (PBS) solution. Hydrogel disks of 10 mm in diameter were placed in 37°C low pH solution for 24 h, weighed in air and a nonsolvent, heptane, then placed in 37°C high pH buffer for 24 h. At the end, the disks were again weighed in air and heptane.

Potentiometric Titration. To determine the MAA content of the hydrogels, a 3.5 mg/mL solution of microgels in deionized water was titrated to pH 11.5 using 0.2 N NaOH (standardized with potassium hydrogen phthalate) at 25°C with constant stirring. pH was measured with a Mettler-Toledo SevenEasy™ (Columbus, OH) pH probe and was recorded when the pH reached a steady value ($\pm$0.01 pH units in three consecutive measurements over 5 min). The equivalence point was used in conjunction with a charge balance to determine the amount of MAA present in each formulation.

Cytotoxicity Study. The cytotoxic effect of the microgels was evaluated using a CellTiter 96® Aqueous One Solution Cell Proliferation Assay (Promega, Madison, WI). Microgel concentrations ranged from 1.25 to 10 mg/mL in Dulbecco's modified Eagle medium (DMEM) without phenol red; studies were completed with human colon adenocarcinoma Caco-2, mucus-secreting HT29 MTX, and murine fibroblast L929 cells. Cells were incubated with microgels for 2 h at 37°C and 5% CO_2, and then the microgel solution was removed. MTS assay was added to the wells and incubated for 90 min at the same conditions before absorbance measurements were made at 490 nm using a Bio-Tek Synergy™ HT multimode plate reader (Winooski, VT).

Caco-2 and L929 cells were obtained from American Type Culture Collection (ATCC, Rockwell, MD) and HT29-MTX cells, a subpopulation of HT29 cells that were adapted to 10^{-6} M methotrexate (MTX),[34] were a gift from Dr. Thecla Lesuffleur, INSERM, Paris, France. All cell lines were cultured in DMEM (Mediatech, Herndon, VA) supplemented with 10% heat-

Table I. P(MAA-*co*-NVP) Hydrogel Formulations

Formulation nanogel %, crosslinker	Nanogel weight %	Crosslinker
0 w t%, TEGDMA	0	TEGDMA
1 wt %, TEGDMA	1	TEGDMA
2 wt %, TEGDMA	2	TEGDMA
5 wt %, TEGDMA	5	TEGDMA
0 wt %, PEGDMA	0	PEGDMA
1 wt %, PEGDMA	1	PEGDMA
2 wt %, PEGDMA	2	PEGDMA
5 wt %, PEGDMA	5	PEGDMA

inactivated fetal bovine serum (Cambrex, East Rutherford, NJ), 1% nonessential amino acids (Mediatech), 100 U/mL penicillin, and 100 μg/mL streptomycin (Mediatech).

Loading and Release Studies. Microgels were loaded by equilibrium partitioning postsynthesis with two models, bovine serum albumin (BSA) (Sigma-Aldrich) and FITC-dextran (MW 3000–5000, Sigma-Aldrich). Microgels were incubated at 37°C overnight in a 0.5 mg/mL BSA or FITC-dextran solution of pH ~5.5 at a ratio of 7:1 microgel:model therapeutic by weight. The microgels were then collapsed by addition of 1 N HCl, followed by a wash with 0.2 N HCl and recovery by vacuum filtration. The microgels were lyophilized and stored in a desiccator. Protein loading was evaluated with a MicroBCA assay (Pierce-Thermo, Rockford, IL) and FITC-dextran loading by fluorescence.

Release studies were completed in pH 7.4 PBS buffer at 37°C at a microgel concentration of 0.6 mg/mL buffer. Samples were taken at 0, 5, 10, 15, 30, 60, and 120 min. Protein or FITC-dextran concentration was evaluated in the same manner as the loading study.

RESULTS AND DISCUSSION

Eight different formulations were synthesized, as listed in Table I. Nanogel weight percent is the feed percentage. The formulations will be referred to henceforth by their descriptive name in Table I. All films had an opaque appearance and were glassy and brittle when dry at room temperature.

Microgel Morphology

Hydrogel films were dried and crushed into microgels resembling a fine, white powder. SEM images of dried microgels, as seen in Figure 1, showed the wide polydispersity of size and morphology attributed to the crushing of the hydrogel film. At least two dimensions of the microgels are <75 μm as ensured by the sieving process, but other dimension of the microgel may vary due to the inability to control particle size and shape during the crushing of the film. Comparing Figures 1A and B, there is no observable distinction of the nanogels within the microgel. There is also no noticeable difference in morphology between TEGDMA and PEGDMA crosslinking agents, shown in Figure 1A and C, respectively.

To confirm the nanogels remain within the microgels throughout synthesis and purification, the nanogels were labeled with NBD-Cl, which binds to primary amines present on the surface of the nanogels. Upon reaction with the amine, the NBD-Cl becomes a fluorescent compound ($\gamma_{ex} = 464$ nm, $\gamma_{em} = 512$ nm), effectively labeling the nanogels.[35] Fluorescent microscopy was used to evaluate the fluorescence of microgels containing 0 and 5 wt % nanogels before and after reaction with NBD-Cl. As shown in Figure 2, microgels containing no particles exhibited only a background level of fluorescence, while there was a definite increase in the fluorescence intensity of microgels containing 5 wt % nanogels after reacting with NBD-Cl.

FT-IR Spectroscopic Analysis

The FTIR spectra for all formulations are shown in Figure 3. The characteristic IR band of the nanogels was indistinguishable as it was masked by the wide band in the 2800–3100 cm^{-1} range attributed to the stretching mode of hydrogen-bonded carboxylic acid dimers.[36] However, several important bands appear in the 1200–2000 cm^{-1} range, shown in Figure 3. In the carbonyl-stretching region, the band at 1700 cm^{-1} is attributed to the carbonyl of the carboxylic acid, and the band at 1725 cm^{-1} is indicative of complexation between the hydroxyl group of the acid and carbonyl of the PNVP.[36] Similarly, the stretching band at 1680 cm^{-1} is attributed to the carbonyl of PNVP and is shifted to 1640 cm^{-1} when hydrogen bonding is present.[37] The band at 1290 cm^{-1} is ring C—N stretching coupled with ring CH_2 wagging in PNVP.[37]

Using the reported reactivity ratios of $r_1 = 0.56$ and $r_2 = 0.04$ for MAA and NVP respectively,[38] an equimolar feed ratio of MAA:NVP should result in an approximately alternating structure of 60:40 MAA:NVP as calculated by the copolymer equation. Copolymer molar compositions were calculated based on peak absorbance relative to a standard band absorbance.[33] Using this method, the calculated molar ratios were comparable to the

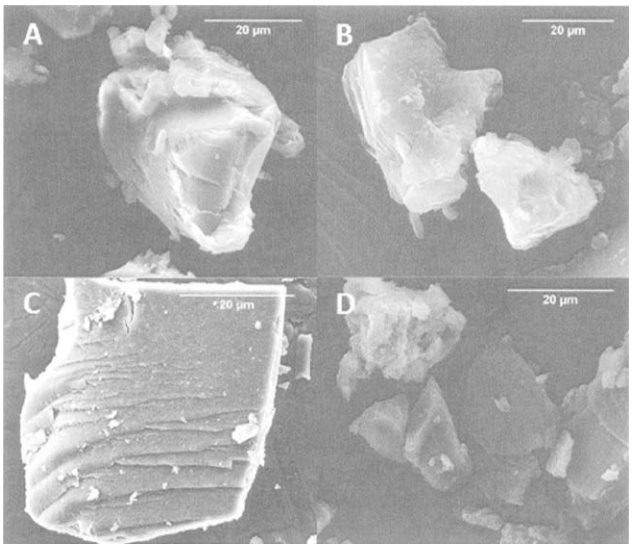

Figure 1. Representative SEM micrographs of crushed P(MAA-*co*-NVP) microgels. Gels were crushed and sieved to <75 μm. A) 0 wt % nanogels, TEGDMA crosslink; B) 5 wt % nanogels, TEGDMA crosslink; C) 0 wt % nanogels, PEGDMA crosslink; D) 5 wt % nanogels, PEGDMA crosslink (Scale bar = 20 μm).

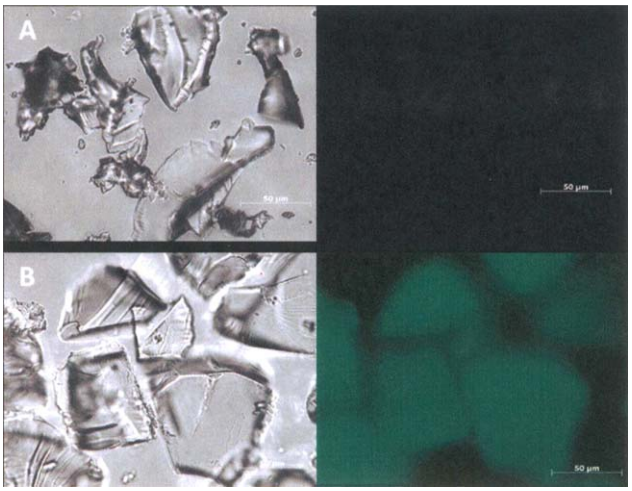

Figure 2. Brightfield (left) and fluorescent microscopy (right) images of crushed P(MAA-*co*-NVP) microgels with PEGDMA crosslinks. A) Film with no nanogels reacted with NBD-Cl; B) Film with 5 wt % nanogels reacted with NBD-Cl (Scale bar = 50 μm). [Color figure can be viewed in the online issue, which is available at wileyonlinelibrary.com.]

theoretical compositions, as shown in Table II. As the copolymer equation does not take into account the effect of the crosslinking agent, the calculated values are reasonable. The incorporation of nanogels into the feed appears to have little to no effect on reactivity.

TGA Analysis

The TGA results from the TEGDMA microgels are shown in Figure 4A and the PEGDMA microgels in Figure 4B. TGA indicated that all formulations have a similar degradation profile, suggesting the same degradation mechanism. The first stage of degradation, beginning at about 60°C and accounting for approximately 6% weight loss, may be attributed to the loss of water and smaller molecules or oligomers.[39] The second stage of degradation begins at about 160–175°C and accounts for up to 5% weight loss. This loss is likely anhydride formation and some decarboxylation within the MAA, resulting in release of water and carbon dioxide.[40] It is interesting to note that this loss occurs at higher temperatures relative to that of pure PMAA, as has been observed by Polacco et al. with PMAA/PVP complexes.[41] The nanogels undergo significant degradation in this region, which may also contribute to the weight loss. The transition occurred approximately 10°C earlier in gels with PEGDMA crosslinker than in gels with TEGDMA crosslinker. The crosslinker likely affects intramolecular bonding within the gel, causing variances in stability as a function of temperature. All formulations showed massive degradation from 300 to 500°C, with a maximum at about 430°C. This is a result of the decomposition of the polymer backbone primarily into monomer units, but also some oligomers.[39,41]

Swelling Studies

Dynamic swelling studies were conducted to evaluate the hydrogels' response to pH variation on a short time scale (10 min/buffer). Weight swelling ratios were calculated using eq. (1), where W_D is the dry weight of the hydrogel disk and W_S is the swollen weight.

$$q = \frac{W_S}{W_D} \quad (1)$$

As shown in Figures 5A and B, all formulations exhibit an increase in weight swelling ratio at pH values greater than ~5, which is expected as the pKa of methacrylic acid is approximately 4.8.[42] Beyond the pKa of MAA, the carboxylic acid groups are ionized, and ionic repulsion drives the swelling of the hydrogel to weight swelling ratios ranging from 1.3 to 1.6. It was especially important to evaluate if the hydrogels swell at low pH, since the nanogels would be ionized below pH ~6.

The pH response of formulations with TEGDMA crosslinker, shown in Figure 5A, is affected by the incorporation of nanogels as demonstrated by greater swelling ratios at low pH in formulations with higher nanogel content. This is because the nanogels are ionized at low pH and swelling facilitated by ionic repulsion allows increased imbibition of solution, resulting in increased weight swelling ratios. Around pH 5, however, the 2 wt % TEGDMA gels reach greater swelling ratios than the 5 wt % TEGDMA gels as the cationic nanogels collapse upon exposure to high pH solution, resulting in a decrease in weight swelling ratio that is more apparent with greater nanogel content.

On the other hand, formulations with PEGDMA crosslinker are not as sensitive to the nanogel incorporation and the weight swelling ratios are similar regardless of nanogel content, shown in Figure 5B. In the case of the PEDGMA gels, the longer crosslinker allows the network to be swollen to the point where any weight loss resulting from the collapse of nanogels is negligible. This characteristic may have unique applications in oral drug delivery as it allows nanogel incorporation while minimizing pH-dependent swelling variations.

Equilibrium swelling studies were conducted to obtain the maximum weight swelling ratio of the gels and calculate the swollen mesh size. All formulations had a weight swelling ratio ~1.3 in the 0.1 N HCl buffer (data not shown). For many formulations, including all of the TEGDMA gels, swollen weights at pH 7.4 could not be measured due to the fragility and rupture of the gels prior to reaching equilibrium. For those that reached equilibrium swelling, the mesh size was calculated using the Peppas–Merrill equation. Weight swelling ratios at pH 7.4 for the PEGDMA gels, as well as the calculated swollen mesh size, are reported in Table III. The swollen mesh sizes ranged from ~21 to 35 nm for the PEGDMA gels. The equilibrium weight swelling ratios of the PEGDMA gels are much greater than the dynamic swelling weight ratios at pH 7.4, indicating some tortuosity present in the hydrogel that retards swelling on a short time scale. This may be due to regions of crystallinity or the glassiness of the hydrogel in a dried state.

Potentiometric Titration

Potentiometric titration studies were completed with crushed microgels to determine the actual MAA incorporation in each formulation and whether the crosslinking agent or addition of nanogels had any effect. As shown in Table II, formulations with the TEGDMA crosslinker had 46–50 mol % MAA, which was the inverse of what was calculated from the FTIR spectra.

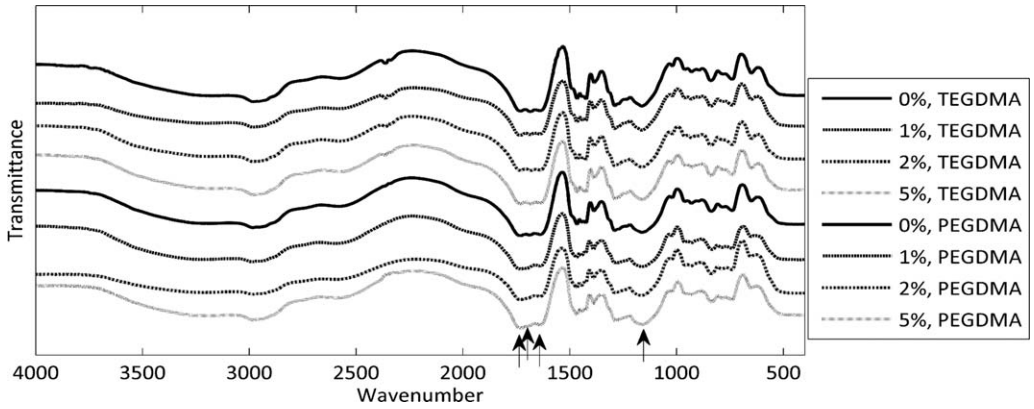

Figure 3. FT-IR spectra of crosslinked P(MAA-*co*-NVP) copolymers with encapsulated nanogels at varying weight percentages (0–5 wt %) pressed in a KBr disk. Crosslinking was achieved with either poly(ethylene glycol) (400) dimethacrylate or tetra(ethylene glycol) dimethacrylate at 1 mol %. Arrows mark bands of interest.

However, the lower relative content of MAA explains why these formulations exhibit some swelling at a low pH as observed in the dynamic swelling studies, since the hydrophilicity of the NVP dominates. On the other hand, formulations with the PEGDMA crosslinker had 53–66 mol % MAA, which was in close agreement with what was calculated from the FTIR spectra though a bit higher for formulations that contained nanogels. The higher relative amount of MAA in the PEGDMA gels explains the dynamic swelling profile of these gels; the swelling response is controlled by the ionization of MAA rather than the hydrophilicity of NVP. As in the case of the FTIR analysis, the amount of crosslinker and nanogels incorporated was not taken into account, so some error is expected. Additionally, the polycationic nanogels are ionized at pH values $<\sim 6$, but the charge of this species was ignored due to the low relative content.

Cytotoxicity

Cytotoxicity studies were performed with various microgel concentrations to find the maximum concentration that Caco-2 and murine fibroblast L929 cells (data not shown) could withstand without disruption to metabolic activity. Figures 6A and B shows Caco-2 cell viability relative to a positive control without microgels. Viability greater than 80% is considered acceptable in our evaulation. For all formulations, concentrations >1.25 mg/mL caused significant disruption to cell metabolic activity. This may reflect a chemical impediment of cellular activity due to a reduction in pH resulting from higher concentrations of charged functional groups, or a physical impediment of cellular activity due to the density of the sedimenting particles covering the cell monolayer. The trend suggests that higher incorporation of nanogels may cause loss of cell viabilty; this is in agreement with

Table II. Molar Ratios of MAA and NVP in P(MAA-*co*-NVP) Microgels Determined by FTIR and Potentiometric Titration

	MAA		NVP	
	FTIR (%)	Titration (%)	FTIR (%)	Titration (%)
0%, TEGDMA	53	47	47	53
1%, TEGDMA	55	50	45	50
2%, TEGDMA	53	46	47	54
5%, TEGDMA	53	48	47	52
0%, PEGDMA	53	53	47	47
1%, PEGDMA	55	61	45	39
2%, PEGDMA	58	66	42	34
5%, PEGDMA	56	62	44	38

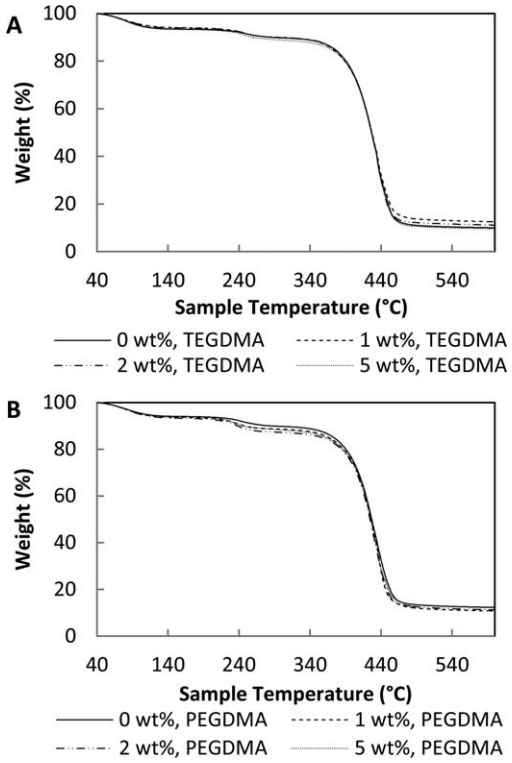

Figure 4. TGA curves of P(MAA-*co*-NVP) copolymers with TEGDMA (A) or PEGDMA (B) crosslinks and 0–5 wt % encapsulated nanogels. 15 mg samples were run at 10°C/min from 40 to 600°C under nitrogen gas.

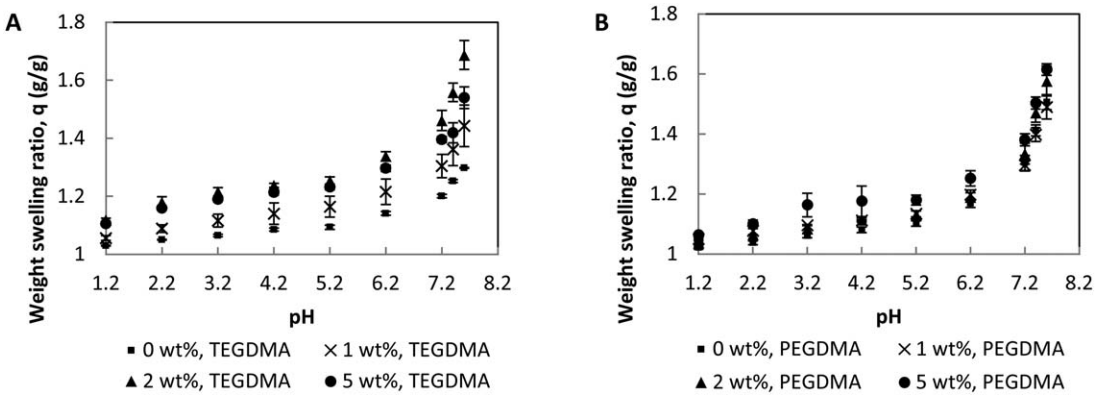

Figure 5. Weight swelling ratio of crosslinked P(MAA-*co*-NVP) hydrogel disks in response to dynamic change in buffer pH. Hydrogels were crosslinked with TEGDMA (A) or PEGDMA (B) and contained 0–5 wt % nanogels. Studies were completed in DMGA/NaOH or HCl buffer with 0.1 M NaCl at 37°C ($N = 3$).

reports of tocixity associated with cationic polymers.[43] This leads us to believe that the charged functional groups within the polymer play a role in the cytotoxicty results, but at low concentrations this effect is not very pronounced. Additionally, for drug delivery applications, it is not likely that local concentrations higher than 1.25 mg/mL would exist.

Loading and Release of Model Therapeutic

Two formulations were chosen to proceed with loading and release studies based on results from the aforementioned characterization studies. The PEGDMA hydrogels with 0 and 5 wt % nanogels were used to evaluate potential influence of nanogel presence on ability to load and release model therapeutics. It was hypothesized that in a loading buffer of pH ~5.5, the P(MAA-*co*-NVP) matrix and nanogels should both undergo swelling due to partial ionization. In that case, there is a possibility that the therapeutic could partition into the nanogels, which would remain collapsed at a high pH ~7.4 and fail to release the therapeutic. This could have applications in both drug delivery and protein separations.

The first therapeutic tested was BSA, a large (66.5 kDa) model protein. Loading efficiency was calculated by eq. (2) and weight efficiency was calculated by eq. (3), where c_o is the initial protein concentration, c_f is the final protein concentration, mass_o is the initial mass of protein in solution, mass_f is the final mass of protein in solution, and mass_p is the mass of polymer in solution.

$$\text{Loading Efficiency} = \frac{c_o - c_f}{c_o} \times 100 \quad (2)$$

$$\text{Weight Loading Efficiency} = \frac{\text{mass}_o - \text{mass}_f}{\text{mass}_o - \text{mass}_f + \text{mass}_p} \times 100 \quad (3)$$

As shown in Figure 7, the weight-loading efficiencies were very similar regardless of nanogel content. Though the loading and weight efficiencies of BSA were lower than desired at ~40–45% and ~5.5–5.6%, respectively, they were comparable to those reported for similar hydrogel systems with large proteins.[44]

The release of BSA from microgels was calculated relative to the total weight of therapeutic based on the weight-loading efficiency for each formulation. For both formulations, a burst release was observed in pH 7.4 buffer, reaching a maximum of ~50–60% in approximately 20 min as shown in Figure 8A. We can infer that the therapeutic was not loaded into the nanogels in the 5 wt % formulation, since we would expect to see lower release relative to that of the 0 wt % formulation as the nanogels would remain collapsed at pH 7.4. This disproves the hypothesis that the nanogels could be loaded simultaneously at pH 5.5, but there is a possibility that the loading procedure could be modified to achieve simultaneous loading of nanogels and microgels in the 5 wt % formulation.

With respect to the 0 wt % formulation, the percent release of BSA was low compared to reported release of other proteins from comparable systems.[44] This is likely due to a combination of the large size of BSA restricting diffusion along with some surface loading rather than partitioning within the hydrogel. A small amount of the protein is likely removed from the particle surface during the wash steps following the loading procedure, which would result in artificially high loading efficiencies and seemingly low percent release. Charge repulsion between the protein and microgel may also factor into the low release percentages; at pH 7.4 both the BSA and microgels carry a negative charge, which may impede diffusion of BSA from the microgel.

To determine if the size of the therapeutic was affecting partition loading and release, a smaller model therapeutic, FITC-dextran (3–5 kDa) was also evaluated. The loading efficiencies were higher for this model, at around ~65–67% loading efficiency as shown in Figure 7, while the weight-loading efficiencies were nearly the same as BSA at ~5.3–5.6%. Again there was little difference between the 0 and 5 wt % formulations.

Table III. Equilibrium Weight Swelling Ratios and Calculated Swollen Mesh Size of P(MAA-*co*-NVP) 10 mm Disks ($N = 3$)

Formulation	$q_{pH\ 7.4}$ (g/g)	Swollen mesh size (nm)
0 wt % PNP, PEGDMA	N/A[a]	N/A[a]
1 wt % PNP, PEGDMA	14.3 ± 0.8	25–35
2 wt % PNP, PEGDMA	14.7 ± 1.8	25–35
5 wt % PNP, PEGDMA	11.7 ± 0.5	21–22

[a] Could not be determined due to disk rupture.

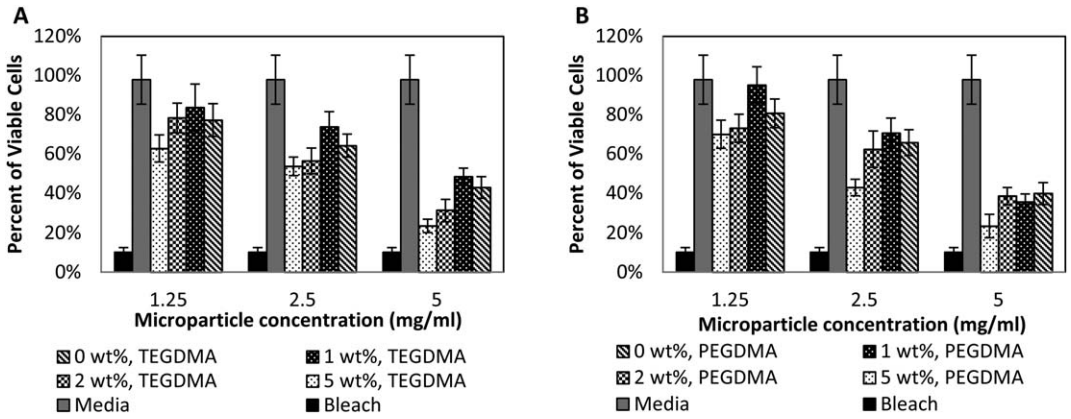

Figure 6. Evaluation of cell viability after microgel exposure using an MTS cell proliferation assay (Promega). Caco-2 human colorectal adenocarcinoma cells were incubated with microgel solutions ranging from 1.25 to 5 mg/mL in culture media for 2 h. Following removal of the microgels, the MTS assay was allowed to incubate for 90 min. Percent viable cells is relative to the positive control (culture media only, gray bar). Microgels were crosslinked with TEGDMA (A) or PEGDMA (B) and contained 0–5 wt % nanogels ($N = 3$).

These efficiencies were comparable to a similar system loaded with a smaller protein.[45]

As in the case of BSA, both the 0 and 5 wt % formulations showed similar release profiles and percentages, disproving the hypothesis that the nanogels would be loaded with model therapeutic. The release of FITC-dextran in pH 7.4 buffer, shown in Figure 8B, was unexpectedly low at 20–25% release for the 0 wt % formulation. It was anticipated that the 0 wt % nanogel formulation would exhibit a much higher percent release than the 5 wt % nanogel formulation, since the therapeutic could have been contained within the nanogels in the 5 wt % formulation, but the data did not support this. This suggests that the model therapeutic is not partitioning into the nanogels, or that the therapeutic diffused from the nanogels as the microgels collapsed in the acidified environment. As accurate fluorescence measurements could not be obtained after collapsing the particles by acidification of the solution, it is possible that some of the loaded FITC-dextran was forced out of the microgels as the structure collapsed and the actual loading efficiencies were lower, causing depressed release efficiencies. It is also possible that hydrogen bonding between the microgel and polysaccharide chains inhibited adequate loading and release.

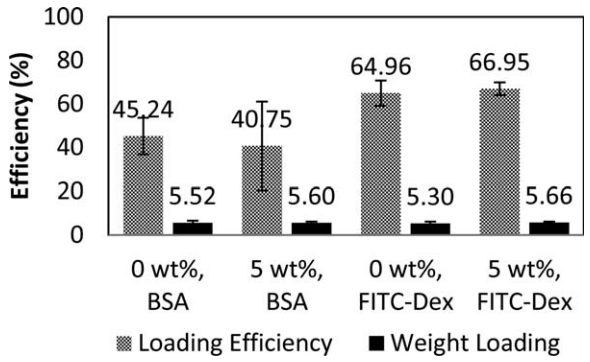

Figure 7. Loading efficiencies of P(MAA-*co*-NVP) microgels with PEGDMA crosslinker and 0 or 5 wt % nanogels. Bovine serum albumin (BSA, MW 66.5 kDa) and FITC-dextran (FITC-Dex, MW 3–5 kDa) were loaded into the microgels. Loading efficiency was based on amount of protein or dextran loaded into microgels relative to initial amount in solution. Weight-loading efficiency is the weight of loaded protein or dextran relative to the total weight of microgel and protein or dextran. Microgels were loaded over 24 hours ($N = 3$).

CONCLUSIONS

Formulations with two different crosslinking agents and varying cationic nanogel content were synthesized by UV-initiated bulk free radical polymerization. The microgels have similar morphology across formulations and retain the nanogels through synthesis and purification, as shown by fluorescent microscopy. Copolymer composition based upon feed ratio and FTIR is in good agreement at approximately 60:40 MAA:NVP and does

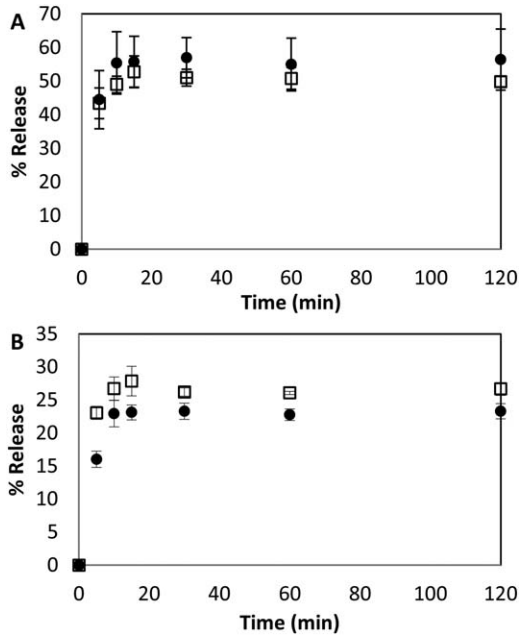

Figure 8. Release of model therapeutics from P(MAA-*co*-NVP) microgels with PEGDMA crosslinker in pH 7.4 PBS buffer at 37°C over 2 hours. Error bars are standard deviation ($N = 3$). Microgels encapsulated either 0 (●) or 5 wt % (□) nanogels. A) Release of bovine serum albumin (MW 66.5 kDa); B) release of FITC-dextran (MW 3–5 kDa).

not vary widely across formulations. However, the swelling behaviors of the gels do indicate some differences, with the TEGDMA hydrogels experiencing higher weight swelling ratios with increased nanogel content while the swelling of the PEGDMA gels are not dependent upon nanogel content, which is favorable for drug delivery applications. Two model therapeutics were loaded into the PEGDMA microgels, but the release of the models was lower than expected in both cases and nanogel content did not affect loading or release efficiency. It is likely that the release is poor due to surface loading rather than equilibrium partitioning with in microgels.

ACKNOWLEDGMENTS

This work was supported by a grant from the National Science Foundation (CBET-1033746). JMK acknowledges support from the National Science Foundation Graduate Research Fellowship Program (DGE-1110007). We wish to thank Dr. Thecla Lesuffleur, INSERM, Paris, France, for the generous gift of the HT29-MTX cell line.

REFERENCES

1. Peppas, N. A.; Hilt, J. Z.; Khademhosseini, A.; Langer, R. *Adv. Mater.* **2006**, *18*, 1345.
2. Peppas, N. A.; Bures, P.; Leobandung, W.; Ichikawa, H. *Eur. J. Pharm. Biopharm.* **2000**, *50*, 27.
3. Jeong, B.; Gutowska, A. *Trends Biotechnol.* **2002**, *20*, 305.
4. Firestone, B. A.; Siegel, R. A. *J. Appl. Polym. Sci.* **1991**, *43*, 901.
5. Kost, J.; Langer, R. *Adv. Drug Deliver. Rev.* **2012**, *64*, 327.
6. Qiu, Y.; Park, K. *Adv. Drug Deliver. Rev.* **2012**, *64*, 49.
7. Hoffman, A. S. *Adv. Drug Deliver. Rev.* **2013**, *65*, 10.
8. Liechty, W. B.; Scheuerle, R. L.; Peppas, N. A. *Polymer* **2013**, *54*, 3784.
9. Gran, M. L. Metal-Polymer Nanoparticulate Systems for Externally-Controlled Delivery. In Chemical Engineering; The University of Texas at Austin: Austin, **2010**.
10. Bajpai, A. K.; Shukla, S. K.; Bhanu, S.; Kankane, S. *Prog. Polym. Sci.* **2008**, *33*, 1088.
11. Tokareva, I.; Minko, S.; Fendler, J. H.; Hutter, E. *J. Am. Chem. Soc.* **2004**, *126*, 15950.
12. Stuart, M. A. C.; Huck, W. T. S.; Genzer, J.; Müller, M.; Ober, C.; Stamm, M.; Sukhorukov, G. B.; Szleifer, I.; Tsukruk, V. V.; Urban, M.; Winnik, F.; Zauscher, S.; Luzinov, I. Minko, S. *Nat. Mater.* **2010**, *9*, 101.
13. Peppas, N. A.; Byrne, M. E. *Bull. Gattefossé*. **2003**, *96*, 23.
14. Martins, A. M.; Alves, C. M.; Kurtis Kasper, F.; Mikos, A. G.; Reis, R. L. *J. Mater. Chem.* **2010**, *20*, 1638.
15. Han, L.-H.; Lai, J. H.; Yu, S.; Yang, F. *Biomaterials* **2013**, *34*, 4251.
16. Gao, T.; Ye, Q.; Pei, X.; Xia, Y.; Zhou, F. *J. Appl. Polym. Sci.* **2013**, *127*, 3074.
17. Xiao, L.; Isner, A. B.; Hilt, J. Z.; Bhattacharyya, D. *J. Appl. Polym. Sci.* **2013**, *128*, 1804.
18. Marambio, O. G.; Pizarro, G. d. C.; Jeria-Orell, M.; Geckeler, K. E. *J. Appl. Polym. Sci.* **2009**, *113*, 1792.
19. Tokarev, I.; Minko, S. *Adv. Mater.* **2010**, *22*, 3446.
20. Kayitmazer, A. B.; Seeman, D.; Minsky, B. B.; Dubin, P. L.; Xu, Y. *Soft Matter.* **2013**, *9*, 2553.
21. Gernandt, J.; Hansson, P. *Soft Matter.* **2012**, *8*, 10905.
22. Yigit, C.; Welsch, N.; Ballauff, M.; Dzubiella, J. *Langmuir* **2012**, *28*, 14373.
23. Liu, J.; Chen, G.; Guo, M.; Jiang, M. *Macromolecules* **2010**, *43*, 8086.
24. Motornov, M.; Roiter, Y.; Tokarev, I.; Minko, S. *Prog. Polym. Sci.* **2010**, *35*, 174.
25. White, E. M.; Yatvin, J.; Grubbs, J. B.; Bilbrey, J. A.; Locklin, J. *J. Polym. Sci., Part B: Polym. Phys.* **2013**, *51*, 1084.
26. Fleige, E.; Quadir, M. A.; Haag, R. *Adv. Drug Deliver. Rev.* **2012**, *64*, 866.
27. Schoener, C. A.; Hutson, H. N.; Peppas, N. A. *J. Biomed. Mater. Res. A* **2013**, *101A*, 2229.
28. Welsch, N.; Becker, A. L.; Dzubiella, J.; Ballauff, M. *Soft Matter.* **2012**, *8*, 1428.
29. Chapel, J. P.; Berret, J. F. *Curr. Opin. Colloid Interface Sci.* **2012**, *17*, 97.
30. Knipe, J. M.; Peters, J. T.; Peppas, N. A. *Nano. Today.* **2013**, *8*, 21.
31. Satarkar, N. S.; Biswal, D.; Hilt, J. Z. *Soft Matter.* **2010**, *6*, 2364.
32. Döring, A.; Birnbaum, W.; Kuckling, D. *Chem. Soc. Rev.* **2013**, *42*, 7391.
33. Pekel, N.; Sahiner, N.; Guven, O.; Rzaev, Z. M. O. *Eur. Polym. J.* **2001**, *37*, 2443.
34. Lesuffleur, T.; Porchet, N.; Aubert, J.-P.; Swallow, D.; Gum, J. R.; S. Kim, Y.; Real, F. X.; Zweibaum, A. *J. Cell. Sci.* **1993**, *106*, 771.
35. Ghosh, P. B.; Whitehouse, M. W. *Biochem. J.* **1968**, *108*, 155.
36. Lee, J. Y.; Painter, P. C.; Coleman, M. M. *Macromolecules* **1988**, *21*, 954.
37. Zhu, X.; Lu, P.; Chen, W.; Dong, J. *Polymer* **2010**, *51*, 3054.
38. Bianco, G.; Gehlen, M. H. *J. Photochem. Photobiol. A* **2002**, *149*, 115.
39. Loría-Bastarrachea, M. I.; Herrera-Kao, W.; Cauich-Rodríguez, J. V.; Cervantes-Uc, J. M.; Vázquez-Torres, H.; Ávila-Ortega, A. *J. Therm. Anal. Calorim.* **2010**, *104*, 737.
40. Ho, B.-C.; Lee, Y.-D.; Chin, W.-K. *J. Polym. Sci. Part A: Polym. Chem.* **1992**, *30*, 2389.
41. Polacco, G.; Cascone, M. G.; Petarca, L.; Peretti, A. *Eur. Polym. J.* **2000**, *36*, 2541.
42. Blanchette, J.; Peppas, N. A. *Ann. Biomed. Eng.* **2005**, *33*, 142.
43. Fischer, D.; Li, Y.; Ahlemeyer, B.; Krieglstein, J.; Kissel, T. *Biomaterials* **2003**, *24*, 1121.
44. Carr, D. A.; Gomez-Burgaz, M.; Boudes, M. C.; Peppas, D. N. A. *Ind. Eng. Chem. Res.* **2010**, *49*, 11991.
45. Carr, D. A.; Peppas, N. A. *J. Biomed. Mater. Res. A* **2009**, *92A*, 504.